In situ structural investigation of Fe-S-Si immiscible liquid system and evolution of Fe-S bond properties with pressure

Guillaume Morard, C. Sanloup, B. Guillot, G. Fiquet, M. Mezouar, J. P. Perrillat, G. Garbarino, K. Mibe, T. Komabayashi, K. Funakoshi

In situ structural investigation of Fe-S-Si immiscible liquid system and evolution of Fe-S bond properties with pressure

G. Morard,[1,2,3,4] C. Sanloup,[3,5,6] B. Guillot,[7] G. Fiquet,[3,4] M. Mezouar,[2] J. P. Perrillat,[2] G. Garbarino,[2] K. Mibe,[8] T. Komabayashi,[9,10] and K. Funakoshi[11]

Received 3 March 2008; revised 21 July 2008; accepted 19 August 2008; published 22 October 2008.

[1] Fe-S-Si immiscibility has been investigated using in situ X-ray methods at high pressure and high temperature. An in situ X-ray diffraction study of immiscible liquids for P∼5 GPa and T/Tm∼1.1 has been performed, showing differences in structural properties between S-rich and Si-rich coexisting liquid phases. Moreover, the respective role of S and Si on Fe alloys has been quantitatively investigated in Fe-X liquids (X = S, Si) with 20%wt of light elements. The transition from immiscible to miscible textures has been observed in the ternary mixture by in situ X-ray radiography for the Fe-18wt%S-8.5wt%Si (Fe-28.8at%Si-11.9at%S) sample composition between 12 and 16 GPa. Closure of the miscibility gap occurs in the same pressure range as the Fe-S eutectic liquid evolves toward a compact structure. By working within the framework of the hard sphere (HS) fluid commonly used in liquid state theory, we show that the equation of state (EOS) for additive HS reproduces very well the compressibility of Fe-Si alloys measured in the 0–5 GPa pressure range, whereas that of Fe-S alloys behave quite differently, with a high degree of covalency. However it is also stressed that at higher pressures (P > 15 GPa) liquid Fe-S adopts a structure close to that exhibited by Fe-Si alloys, a feature which suggests that the compressibility of the two alloys should behave similarly at very high pressure due to transition of S behaviour from covalent to interstitial. Hence for Fe-S liquid under core conditions, we conclude that the sound velocity in Fe-S alloy is compatible with PREM model.

Citation: Morard, G., C. Sanloup, B. Guillot, G. Fiquet, M. Mezouar, J. P. Perrillat, G. Garbarino, K. Mibe, T. Komabayashi, and K. Funakoshi (2008), In situ structural investigation of Fe-S-Si immiscible liquid system and evolution of Fe-S bond properties with pressure, *J. Geophys. Res.*, *113*, B10205, doi:10.1029/2008JB005663.

1. Introduction

[2] Although not really quantified, it is a commonly accepted opinion that the Earth's core is composed of iron and nickel alloyed with 5–15 wt% light elements [*Badro et al.*, 2007; *Birch*, 1952]. The range of these light elements, which are siderophile and not too volatile under proto Earth's conditions, is quite restricted: S, Si, O, C and H [*Poirier*, 1994].

[3] In natural metallic systems, a combination of these different elements should be considered. Whereas binary systems have been extensively studied at high pressure and high temperature [*Chudinovskikh and Boehler*, 2007; *Fei et al.*, 2000; *Kuwayama and Hirose*, 2004; *Morard et al.*, 2008; *Ohtani et al.*, 2005, 1984; *Seagle et al.*, 2008; *Wood*, 1993], interactions between light elements diluted in Fe have rarely been studied [*Sanloup and Fei*, 2004; *Siebert et al.*, 2004; *Tsuno et al.*, 2006]. Furthermore, most liquid ternary systems are characterised by a large miscibility gap at ambient pressures (Fe-S-O, Fe-S-Si, Fe-S-C [*Raghavan*, 1988], Fe-Si-O [*Fabrichnaya and Sundman*, 1997]). As metal segregation and chemical equilibration with silicates (solid or liquid) occur at relatively low pressure in planetesimals (size between 3–100 km [*Chabot and Haack*, 2006]) but high temperature (T = 1800 K [*Greenwood et al.*, 2005]), it is important to study the behaviour of iron alloys at low pressure conditions, in the immiscible regime, to determine the effect of light elements on planetesimal differentiation processes.

[1]Institute for Study of the Earth's Interior, Misasa, Tottori, Japan.
[2]European Synchrotron Radiation Facility, Grenoble, France.
[3]Institut de Physique du Globe de Paris, Paris, France.
[4]Institut de Minéralogie et de Physique des Milieux Condensés, Paris, France.
[5]Université Pierre et Marie Curie-Paris 6, Paris, France.
[6]Now at Center for Science at Extreme Conditions and School of Geosciences, University of Edinburgh, Edinburgh, UK.
[7]Laboratoire de Physique Théorique de la Matière Condensée, Université Pierre et Marie Curie-Paris 6, Paris, France.
[8]Earthquake Research Institute, University of Tokyo, Bunkyo-ku, Tokyo, Japan.
[9]Department of Earth and Planetary Sciences, Tokyo Institute of Technology, Okayama, Meguro, Tokyo, Japan.
[10]Geophysical Laboratory, Carnegie Institution of Washington, Washington, District of Columbia, USA.
[11]Spring-8, Japan Synchrotron Radiation Research Institute, Kouto, Hyogo, Japan.

0148-0227/08/2008JB005663$09.00

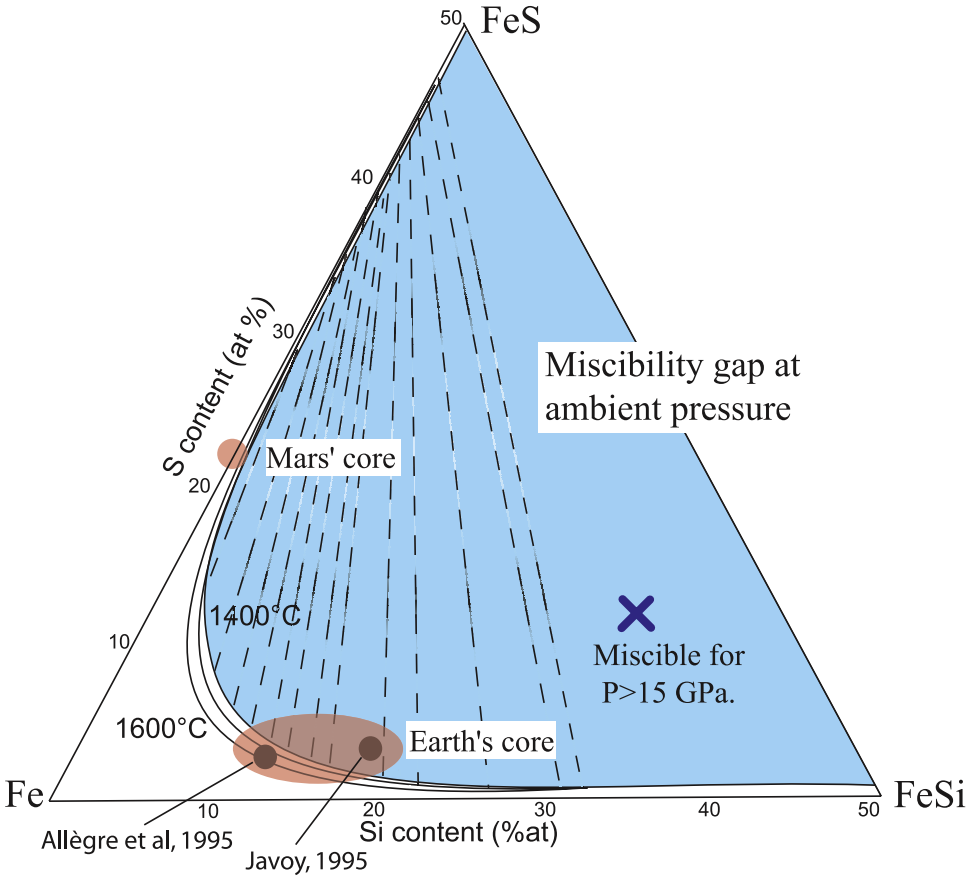

Figure 1. The Fe-S-Si miscibility gap at ambient pressure, from *Raghavan* [1988]. Light blue zone: chemical compositions for which immiscibility occurs. Red areas: possible composition of Earth's and Mars' core deduced from geochemical studies [*Allègre et al.*, 1995; *Javoy*, 1995; *Sanloup et al.*, 1997]. Dashed lines: demixing path followed during decomposition into two immiscible phases. The blue cross indicates the composition Fe-18wt%S-8.5wt%Si (Fe-28.8%atSi-11.9%atS) probed by X-ray radiography and in *Sanloup and Fei* [2004].

[4] Tungsten isotopes indicate that core formation in planetesimals occurred within a few million years of Solar System formation [*Kleine et al.*, 2004]. At the same time, evidence from differentiated meteorites suggests the presence of an early magma ocean on small planetesimals [*Baker et al.*, 2005; *Greenwood et al.*, 2005]. Even if the planetesimal has not been completely molten, migration of S-rich melt through solid silicate is possible by permeable flow [*Yoshino et al.*, 2003]. As the Earth probably built up from such planetesimals, these pre-accretion processes should have left a non negligible imprint on the final geochemical balance. In particular, the existence of liquid iron alloy miscibility gaps might have affected metal segregation mechanisms and consequent element partitioning between metal and silicate phases in planetesimals.

[5] The Fe-S-Si system presents a large miscibility gap at ambient pressure [*Raghavan*, 1988] (Figure 1). As proposed by different geochemical models [*Allègre et al.*, 1995; *Javoy*, 1995], the S and Si contents of the Earth's core lie in this immiscible zone (Figure 1). Concerning Mars' core, a large S content (22.5at% S according to *Sanloup et al.* [1997]) could placed its composition in the immiscible zone by adding only a few percent of Si.

[6] Silicon has a high solubility in pure solid Fe [*Kuwayama and Hirose*, 2004; *Lin et al.*, 2002] and does not disturb liquid Fe structure up to high Si content [*Il'inskii et al.*, 2002; *Kita et al.*, 1982; *Sanloup et al.*, 2002]. Therefore, compressibility is only slightly affected by the presence of Si above 40%at Si [*Sanloup et al.*, 2004]. No evidence is available on the role of Si on the partitioning coefficients between silicate and metallic phases. Thus, it is assumed that the incorporation of Si in the metallic phase does not perturb differentiation processes. On the contrary, S strongly affects the physical properties of iron alloy, such as surface tension [*Iida and Guthrie*, 1994] and bulk modulus [*Sanloup et al.*, 2000]. Furthermore, partitioning coefficients of siderophile elements between silicate and liquid metal are dependent on the S content in the metallic phase [*Jones and Malvin*, 1990; *Righter et al.*, 1997]. In summary, the effect of S and Si on iron alloys at ambient pressure is very different.

[7] The Fe-S-Si system has been studied up to 25 GPa by ex situ analysis on quenched samples [*Sanloup and Fei*, 2004] which indicate a closure of the miscibility gap at high pressure. Recently, an in situ investigation of Fe-FeS liquids has shown structural evolution of the eutectic liquid toward

Table 1. Composition of Quenched Phase of Fe-25%at S-25%at Si Analysed After in situ X-ray Diffraction Experiment (4.5 GPa and 1900 K) Using SEM

	Fe (at%)	S (at%)	Si (at%)	O (at%)
S-rich phase	48.7	50.23	0.02	1.05
Si-rich phase	73.6	2.31	22.36	1.73

a more compact structure [*Morard et al.*, 2007b] that could be linked with the closure of these miscibility gaps. Therefore, investigating how light elements affect the liquid local structure around Fe may lead to important information about geophysical and geochemical processes.

[8] The effect of light elements on the sound velocity in liquid Fe is crucial to determine the Earth's core composition from seismic data. This approach has been used for the solid inner core by coupling seismic data and in situ inelastic X-ray scattering measurements [*Badro et al.*, 2007]. Based upon density measurements of liquid iron alloys performed at P < 5 GPa, Si has been preferred to S to account for the outer core sound velocity [*Sanloup et al.*, 2004]. But the evolution of structural properties observed between 3 and 17 GPa [*Morard et al.*, 2007b] may suggest a change of the physical properties of Fe-S liquid alloys under Earth's core conditions.

[9] In this study, we will present in section 3 the structural properties of binary mixtures of Fe-20wt% S and Fe-20wt% Si at similar pressure-temperature conditions, and that of Fe-S and Fe-Si coexisting immiscible liquids for P = 4.5 GPa and T = 1900 K. These in situ X-ray diffraction studies provide information regarding the origin of the immiscibility in the Fe-S-Si system. Then, to visualize the closure of the miscibility gap as a function of pressure-temperature conditions, an analysis of the texture by X-ray tomography of the ternary mixture Fe-18wt%S-8.5wt%Si (Fe-28.8at%Si-11.9at%S) up to 16 GPa and 2473 K is reported in section 4. Finally, in section 5, the compressibility and the structure of Fe-S and Fe-Si alloys will be discussed in the theoretical framework of HS fluid models.

2. Experimental Procedures

[10] Employing a Paris Edinburgh press (PEP), in situ X-ray diffraction experiments have been performed on the High Pressure beamline ID27 at ESRF in Grenoble, France [*Grima et al.*, 1995; *Mezouar et al.*, 2005; *Mezouar et al.*, 1999]. The very high brilliance X-ray beam delivered by two in-vacuum undulators was collimated down to 50 × 50 microns (typical values). The X-ray wavelength was fixed to $\lambda = 0.2021$ Å (Ytterbium K-edge) or $\lambda = 0.1582$ Å (Platinum K-edge) using a Si(111) channel cut monochromator. A multi-channel collimator [*Mezouar et al.*, 2002] was used to eliminate most of the X-ray background coming from the sample environment materials. The data were collected using a MAR345 imaging plate system (X-Ray research company GmbH, Nodersted, Germany). The sample-detector distance was calibrated with a LaB_6 standard powder and the diffraction images were treated and integrated using the Fit2D software [*Hammersley et al.*, 1996].

[11] The high-pressure chamber consists of two opposed tungsten carbide anvils which have quasi-conical hollows. We used 7 mm boron epoxy gaskets with a classical set up with graphite cylinder resistive furnace, and a hexagonal boron nitride (hBN) capsule was used as a pressure medium and electrical insulator [*Mezouar et al.*, 1999].

[12] The initial sample was prepared from a mixture of pure Fe, FeS and FeSi powders (Goodfellow) with a composition of Fe-25at% S-25at% Si. The sample quenched from 4.5 GPa and 1900 K exhibits two phases corresponding to the two immiscible liquids. The composition of each quenched phase is given in Table 1. Electron microprobe (EMP) analyses were performed (Centre Camparis, UPMC, Paris) using a Cameca SX50 wavelength dispersive spectrometer (WDS). As the sample and the hBN capsule have been in contact with air before loading, oxygen contamination has occurred and SiO_2 grains have been found on the border of the capsule. This oxygen contamination in leading to a slight change in Si initial content, could explain differences in demixing paths between our results (Table 1) and observations in the literature at ambient pressure (Figure 1, [*Raghavan*, 1988]).

[13] Pressure and temperature were calculated from previously established relationships between electric power and temperature in the cell assembly [*Morard et al.*, 2007a] and from cell parameters of the hBN capsule [*Le Godec et al.*, 2000]. Uncertainties arising from this calibration are estimated to be about 200 K and 1 GPa in temperature and pressure, respectively.

[14] The observation of a diffuse signal around a Q value of 30 nm^{-1} ($2\theta = 4.4$ degrees for 0.1582 Å) in association with the disappearance of diffraction peaks associated with the solid phases were the criterion used to assess the complete melting of the sample. However, some diffraction peaks can still remain, suggesting the possible presence of thermal gradients capable of inducing a convective flow in the sample container.

[15] X-ray radiographic experiments were carried out up to 16 GPa using a Kawai-type, 1500 tons multianvil system installed at BL04B1 [*Utsumi et al.*, 1998], SPring-8, Japan. A direct white x-ray beam, which passes through the anvil gaps and the sample at high pressure (Figure 2), was detected with an X-ray camera. Cell assemblies used for radiographic experiments have been designed for the study of immiscible silicate-H_2O melts [*Mibe et al.*, 2004], and were adapted to higher pressures in this study by using 8/3 octahedra, a Re heater and $LaCrO_3$ thermal insulator (Figure 2). Pressures were determined from the cell volume of internal calibrants (BN and MgO) and temperatures were measured with a W5%Re/W26%Re thermocouple. The composition studied was Fe-18wt%S-8.5wt%Si (Fe-28.8at%Si-11.9at%S), to allow direct comparison with previous quench experiments [*Sanloup and Fei*, 2004]. Due to the axial configuration of the cell-assembly relative to the x-ray beam, with the heater and sample lying along the 110 direction, a significant deformation took place upon compression, resulting in a vertical closure of the x-ray gap due to the strong absorption by the flattened Re heater and $LaCrO_3$ sleeve.

3. In situ X-ray Diffraction of Fe-S-Si Immiscible Liquids

[16] Structural properties of coexisting immiscible Fe-S and Fe-Si phases have been investigated by in situ X-ray

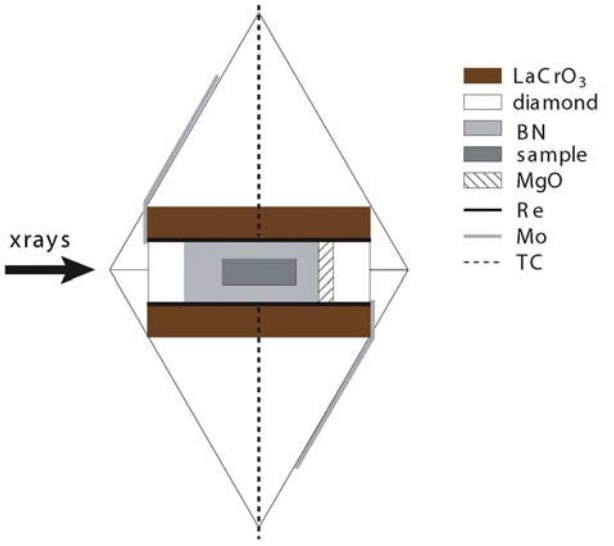

Figure 2. Sketch of the 8/3 cell-assembly used for radiographic experiments. Re: rhenium heater, Mo: molybdenum foil for electrical contact, TC: W-5%Re/W-26%Re thermocouple, inserted around the heater. Octahedron edge length: 8 mm. Sample diameter: 0.5 mm.

diffraction experiment at 4.5 GPa and 1900 K using the PEP. An arrangement within the capsule of the immiscible phases generated by a difference in wetting properties was used to perform this study. By moving the PEP in the X-ray beam, different parts of the capsule loaded with Fe-25at%S-25at%Si sample were probed (Figure 3a). A highly collimated X-ray beam (50 μm $\times$ 50 μm) allows precise spatial scanning of the sample.

[17] Different signals were observed depending on the position of the X-ray beam (Figure 3a). When the X-ray beam probes the central part of the capsule, where the Fe-Si rich phase is observed on quenched samples (Figure 3b), the diffracted signal presents an intense and sharp first diffraction peak around 4° followed by a well defined second peak around 7°. In contrast, when the X-ray beam probes the border of the capsule, where the Fe-S rich phase is located (Figure 3b), the diffracted signal is characterised by a wide and moderately intense first peak with an almost missing second peak.

[18] In order to obtain the pair distribution function g(r) (Figure 4), diffraction signals have been analysed using a previously published method [*Morard et al.*, 2007b]. Since X-ray scattering intensity is proportional to the square of the atomic number, the contribution to the diffraction signal from light elements alloyed with Fe is weak. Thus in the Faber-Ziman formalism [*Faber and Ziman*, 1965; *Vineyard*, 1958] and for the binary mixtures Fe-(20wt%)S and Fe-(20wt%)Si, the Fe-Fe bonds contribute to ~65% of the total signal, and Fe-X bonds to ~30% whereas X-X bonds contribute for only 5%. Therefore, the g(r) characterizes essentially how the Fe-Fe network is perturbed by the presence of light elements while the polymerization of light elements is difficult to decipher.

[19] Difference in local structure is the prime cause of the immiscibility in the Fe-S-Si system. In fact, the Fe-Si liquid phase presents a compact structure with well defined

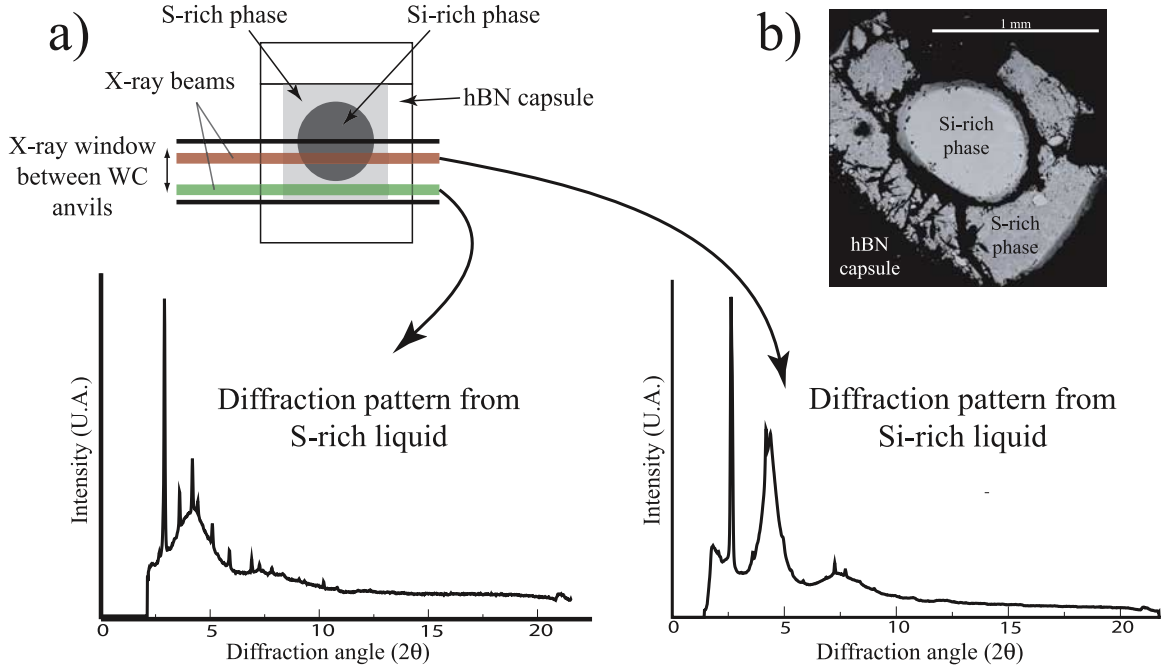

Figure 3. (a) Angle dispersive X-ray diffraction patterns obtained by moving the PEP vertically. Experimental conditions are 4.5 GPa and 1900 K. The sample studied has a global composition of Fe-25%at S-25 %at Si. We can easily discriminate between the two contributions, corresponding to Fe-Si and Fe-S liquids, respectively, and depending on the position of the press. Compositions of both recovered phases are given in Table 1. (b) SEM image of a quenched sample. The Fe-Si phase is the central round domain surrounded by the Fe-S phase wetting the hBN capsule.

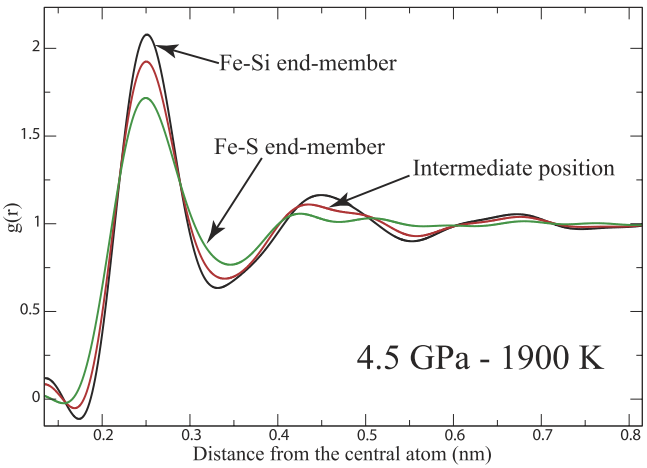

Figure 4. Pair distribution functions g(r), corresponding to the two extreme positions of the PEP (black and green curves) as indicated in Figure 3, and an intermediate position (red curve). For a better comparison, the absolute positions of the CS have been displaced in order to superimpose the position of the first CS exhibited by the Fe-S and Fe-Si alloys.

coordinance spheres (CS) whereas the Fe-S liquid shows only very damped oscillations at distances greater than 0.4 nm (Figure 4). These structures are in good agreement with previous studies [*Sanloup et al.*, 2002; *Urakawa et al.*, 1998]. Two different end-members could be described, with intermediate signals corresponding to mixture of these end-members (Figure 4). However, with the present experimental configuration it is not possible to accurately measure the signal coming from the unmixed phases Fe-S and Fe-Si respectively. Consequently, in order to evaluate more accurately the influence of light elements on the structure of liquid Fe, we have investigated the binary mixtures Fe-S and Fe-Si in separate capsules, at close P-T conditions, and with similar concentrations of light elements (~20%wt).

[20] Figure 5 shows the pair distribution function (pdf) for Fe-20wt%S and Fe-20wt% Si alloys at comparable P-T conditions (4.6 GPa and 1820 K for Fe-20%wt Si; 5.6 GPa and 1400 K for Fe-20% wt S). Indeed, the investigated temperatures correspond approximately to the same T/Tm ratio, where Tm is the eutectic melting temperature (T/Tm ~ 1.1 [*Fei et al.*, 1997; *Kuwayama and Hirose*, 2004]). The small perturbation present on the second CS might be due to termination effect rather than real structural contribution. Its position around 0.38 nm corresponds to theoretical ghost peaks appearance defined by

$$r_{sp1} = r_1 + \Delta r_1 = 0.372 \text{ nm} \quad (1)$$

$$\Delta r_1 \approx \frac{5\pi}{2Q_{\max}} = 0.116 \text{ nm} \quad (2)$$

where r_1 is the position of the first peak [*Waseda*, 1980].

[21] The Fe-20wt% S liquid presents a first peak position at a smaller distance (2.50 Å) than the one exhibited by Fe-20%wt Si (2.56 Å, see Table 2). This shift of the first peak with increasing S content is in good agreement with previous studies of Fe-S alloys with higher S content (from 40at% S to 50at% S, Table 2) [*Sanloup et al.*, 2002; *Urakawa et al.*, 1998; *Vocadlo et al.*, 2000]. This feature is attributed to a stronger Fe-S bond, highlighting its covalent character.

[22] It is generally assumed that Si does not significantly perturb the structure of pure liquid Fe [*Il'inskii et al.*, 2002; *Kita et al.*, 1982; *Sanloup et al.*, 2002] even at concentrations up to 40at% Si [*Kita et al.*, 1982]. Besides, the high solubility of Si in pure solid Fe suggests that Si acts as an interstitial impurity [*Kuwayama and Hirose*, 2004]. Therefore, Fe-Fe networks are relatively undisturbed by the presence of Si and still show a compact structure linked

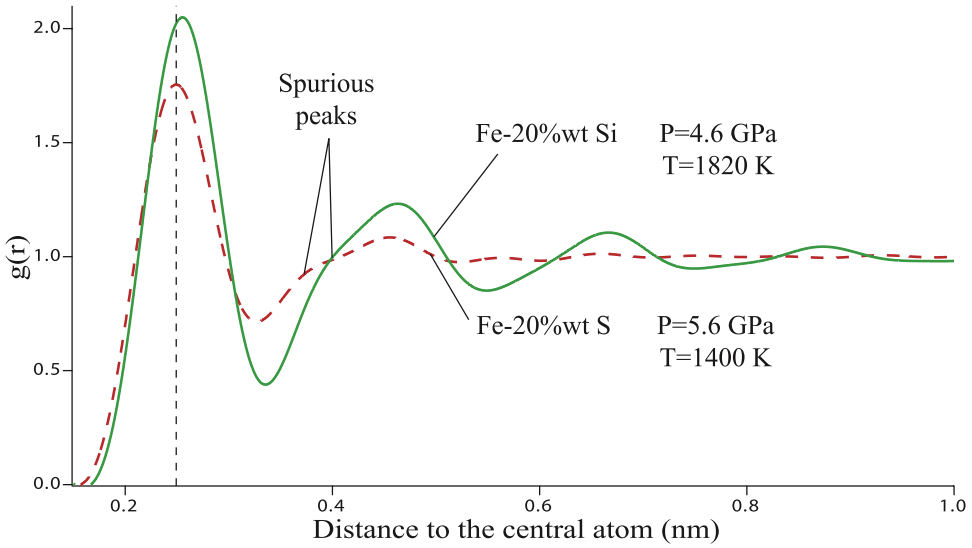

Figure 5. Pair distribution functions g(r) of Fe-20%wt Si (full line) and Fe-20% wt S (dotted line). P-T conditions are indicated in the graph. Spurious peaks are due to termination effect in the data treatment (see text).

Table 2. Position of Maximum of First (r1) and Second (r2) CS of Fe Alloys at Different P-T Conditions From This Study and Other References [*Kita et al.*, 1982; *Morard et al.*, 2007b; *Stolz et al.*, 1994; *Urakawa et al.*, 1998; *Waseda*, 1980]

	P (GPa)	T (K)	r1 (Å)	r2 (Å)	r2/r1	Bibliography
Fe-20%wt S	5.6	1400	2.497	-	-	This study
Fe-20%wt Si	4.6	1820	2.56	4.63	1.809	This study
Fe-20%wt S	16.97	1120	2.477	4.523	1.826	*Morard et al.* [2007]
Pure Fe	Ambient	1823	2.58	4.8	1.860	*Waseda* [1980]
Pure FeS	5.3	1873	2.35	-	-	*Urakawa et al.* [1998]
Pure FeSi	Ambient	1733	2.55	NC	-	*Kita et al.* [1982]
Pure S	Ambient	573	2.054	3.31	1.611	*Stolz et al.* [1994]
Pure Si	Ambient	1733	2.5	5.7	2.28	*Waseda* [1980]

with low compressibility values [*Sanloup et al.*, 2004]. In contrast, the degree of covalency of the Fe-S bond renders S incompatible with the well packed Fe-Si liquid structure.

[23] For pressures greater than 15 GPa, structural evolution occurs in the Fe-FeS system [*Morard et al.*, 2007b], in correlation with Fe-S-Si miscibility gap closure in the 12–15 GPa pressure range [*Sanloup and Fei*, 2004; *Siebert et al.*, 2004]. However, the results concerning melting relationships in the Fe-S-Si system are still controversial, due to the ambiguous interpretation of quenched textures. In this context unambiguous results regarding the closure of the Fe-S-Si miscibility gap are needed. Therefore, in section 4, we investigated the Fe-S-Si system by in situ X-ray tomography up to 16 GPa and 2473 K in order to check the reliability of quenched texture studies.

4. Examining the Miscibility Gap Closure by In situ X-ray Radiography

[24] A sample with a composition of Fe-18wt%S-8.5wt%Si (Fe-28.8%atSi-11.9%atS) was investigated by in situ X-ray radiography at 2, 12 and 16 GPa between 873 K and 2473 K (Figure 6). For each run, temperature was increased at the target pressure while continuously recording X-ray radiographic images. The technique used here (Figure 2) allows the whole sample to be probed to avoid any misinterpretation of the observed texture. The density difference between the two immiscible phases is rather large ($\rho_{\text{Fe-20wt\%S}}$ = 5195 kg.m^{-3} at 2.31 GPa and 1605 K whereas $\rho_{\text{Fe-17wt\%-Si}}$ = 7618 kg.m^{-3} at 1.55 GPa and 1830 K [*Sanloup*, 2000]) and the absorption contrast allows a clear distinction in the miscibility properties (for instance in Figure 6 the Fe-Si phase is related to a darker contrast).

[25] During experiments at 2 and 12 GPa, the formation of two immiscible phases is observed by the presence of darker Fe-Si blobs in lighter Fe-S liquid matrix for temperature above the melting point of both phases. On the contrary, the experiment at 16 GPa does not show heterogeneity up to 2473 K. This temperature is well above the melting temperature of pure end members Fe (~2100 K) [*Boehler et al.*, 2002], FeS (~1800 K) [*Boehler*, 1992] and FeSi (~1900 K) [*Santamaria-Perez and Boehler*, 2008]. One may conclude that the initial composition Fe-18wt%S-8.5wt%Si (Fe-28.8at%Si-11.9at%S) forms only one phase in the liquid state for P > 16 GPa and up to 2473 K. This composition is situated deep within the miscibility gap of the Fe-S-Si system (Figure 1) which suggests that this zone has significantly decreased between the ambient pressure and 16 GPa.

[26] This is direct in situ evidence of the closure of the Fe-S-Si miscibility gap with increasing pressure. It confirms the relevance of earlier studies of quenched textures at high pressure and temperature, in the case of Fe-S-Si system [*Sanloup and Fei*, 2004; *Siebert et al.*, 2004]. This means also that the observation of separated phases in quenched samples is due to the coexistence of two immiscible liquids and not to a diffusion of elements during quenching. The same interpretation has already been applied in the case of the Fe-S-O system [*Tsuno et al.*, 2006].

[27] Closure of the miscibility gap in the Fe-S-Si system implies that S and Si are both compatible with the liquid Fe structure at high pressures. A previous study on the Fe-FeS eutectic liquid [*Morard et al.*, 2007b] has shown that S becomes compatible with a compact structure at P > 15 GPa: a structure similar to that exhibited by Fe-Si liquid at 5 GPa. Therefore, this suggests that S could enter the structure of the Fe-Si liquid to form a Fe-S-Si alloy for P > 15 GPa without substantially altering the local structure. Our explanation of this evolution is a transition from covalent to interstitial behaviour of S in this pressure range. To be more quantitative and to ascertain the effect of light elements on the compressibility of liquid Fe, we have estimated the EOS of Fe-Si and Fe-S alloys in the framework of the HS fluid model.

5. Hard Sphere Model

[28] As a theoretical framework we used a HS model to interpret differences in structural and compression behaviour between Fe-S and Fe-Si liquids. In this framework, a binary mixture (e.g. Fe-Si) is described as a mixture of HS, with fixed diameters. Although very crude this approximation is suitable for liquid metals under pressure where the ion-ion repulsion is the main driving force for atomic packing [*Barker and Henderson*, 1976; *Waseda*, 1980].

[29] Various studies have described the behaviour of HS mixtures [*Mulero et al.*, 2001]. For the so-called additive HS model (AHS) the distance of closest approach (denoted by σ_{ij}) between the centres of two interacting particles, one of the species, *i*, and the other of the species, *j*, is the arithmetic mean of the diameters of both particles σ_i and σ_j. An analytic equation of state known as the Mansoori-Carnahan-Starling-Leland equation [*Mansoori et al.*, 1971], derived from the Percus Yevick integral equation for HS mixtures, has been applied to the Fe-Si alloy to evaluate the evolution of the compressibility with Si content (for a review on the EOS for HS see [*Mulero et al.*, 2001]).

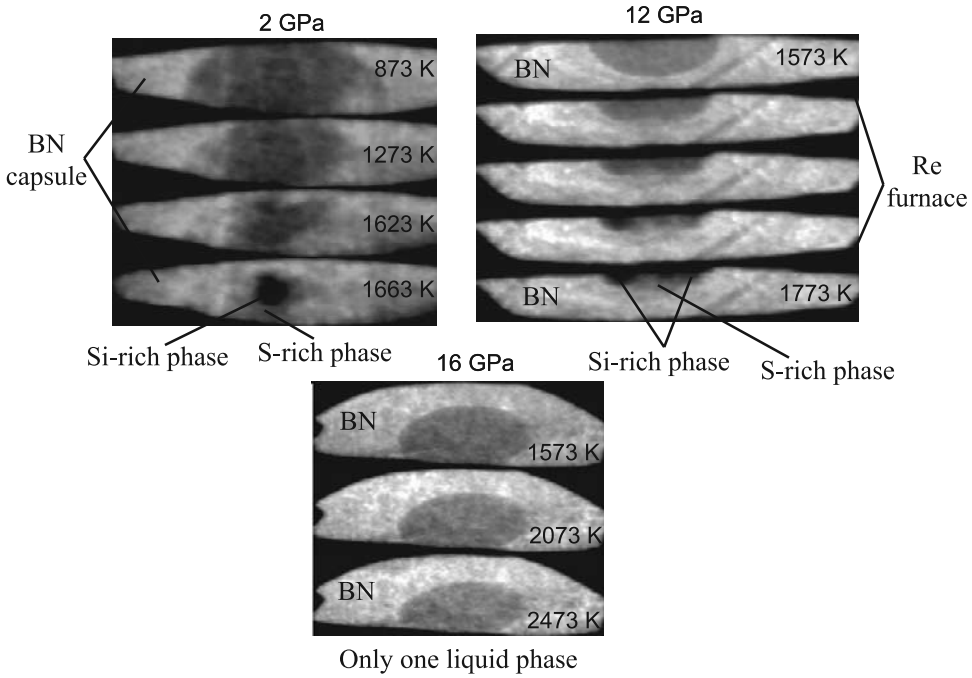

Figure 6. X-ray radiographic images as a function of pressure and temperature from a sample of composition Fe-18wt%S-8.5wt%Si (Fe-28.8%atSi-11.9%atS). Two domains with different X-ray absorption properties are present at 2 and 12 GPa for the highest temperature, whereas only one phase remains at 2200°C and 16 GPa.

The value of the HS diameter assigned to Fe (σ_{Fe}) was chosen by fitting the published pressure-density data for pure liquid Fe [*Anderson and Ahrens*, 1994]. As for σ_{Si}, it was adjusted to best reproduce the pressure-density data for Fe-Si liquid mixtures [*Sanloup et al.*, 2004].

[30] As illustrated in Figure 7, we obtain a good agreement between the compressibility data for Fe-Si alloys and the AHS model. This result is qualitatively important since it suggests that the Fe-Si mixture behaves like a HS mixture and adopts a compact structure at high pressure for Si content up to 40%at [*Kita et al.*, 1982]. (It must be noted that the AHS model does not agree with pure Si density data [*Delisle et al.*, 2006] because of a specific Si-Si interaction not accounted for in the model). This behaviour is compatible with an interstitial dissolution of Si in the pure liquid Fe for limited Si content. In fact, a similar conclusion can be reached from the structural properties of Fe-Si liquid [*Il'inskii et al.*, 2002; *Kita et al.*, 1982; *Sanloup et al.*, 2002], where a compact structure is observed in this system (see the oscillatory behaviour of g(r) at large r in Figure 5).

[31] In the case of Fe-S liquid mixture, the AHS model is unreliable. More precisely, the large rise of the compressibility with increasing S content observed at low pressure [*Sanloup et al.*, 2000] cannot be reproduced with an AHS model (in contrast, the bulk modulus at low pressure of Fe-Si mixtures varies very little with composition). Adding S significantly increases the compressibility and leads to density values greater than the one expected for pure liquid Fe at high pressure.

[32] As previously discussed, under pressure significant changes are observed in the position of the first coordination shell in the Fe-S liquid compared to pure Fe or Fe-Si liquid (Table 2). This evolution could be attributed to the covalent character of the Fe-S bond. Hence, the EOS for non-additive HS (NAHS) mixtures has been used [*Hamad*, 1997]. In this model, the non-additive behaviour is obtained by defining

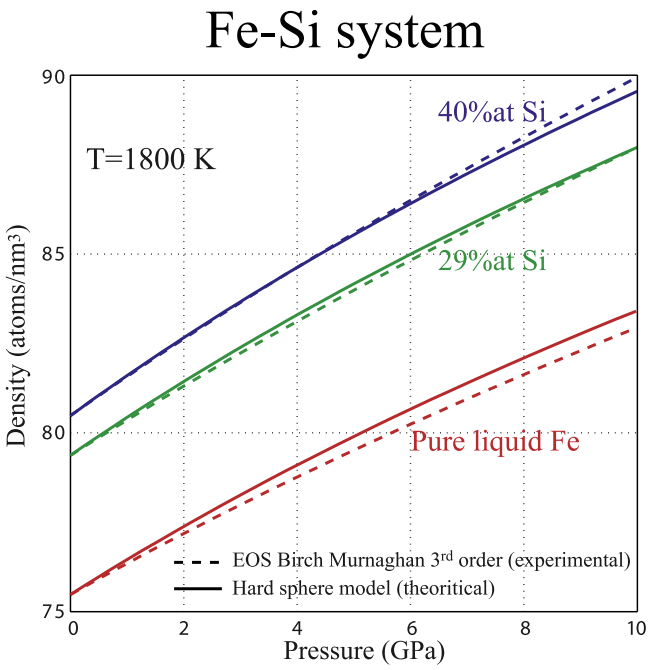

Figure 7. Additive HS EOS [*Mansoori et al.*, 1971] applied to the Fe-Si system compared with experimental data [*Anderson and Ahrens*, 1994; *Sanloup et al.*, 2004]. EOS parameters are the following: σFe = 2.27Å; σSi = 2.08 Å.

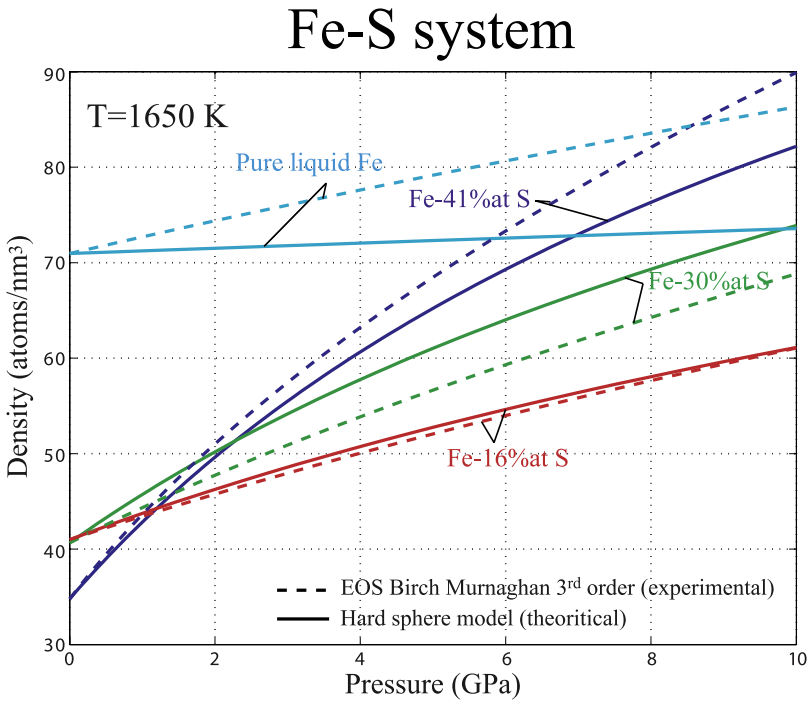

Figure 8. Non additive HS EOS [*Hamad*, 1997] applied to the Fe-S system compared with experimental data [*Anderson and Ahrens*, 1994; *Sanloup et al.*, 2000]. EOS parameters are the following: σFe = 2.55 Å; σS = 2.35 Å; $\Delta = -0.35$.

the distance of closest approach between particles of different species using the following relation:

$$\sigma_{ij} = \left(\sigma_{ii} + \sigma_{jj}\right)\frac{(1+\Delta)}{2} \tag{3}$$

where the parameter Δ quantifies a deviation with respect to the arithmetic mean of HS diameters.

[33] A positive value of Δ, denoting a large repulsion between unlike species, leads to demixing [*Dijkstra*, 1998]. In the case of an Fe-S alloy, we investigated a negative value of Δ, which accounts for the short range ordering [*Hamad*, 1997] induced by a preferential hetero-coordination between Fe and S atoms. This is suggested by a shift of the first coordination shell towards smaller distances in going from Fe-Si mixtures to Fe-S mixtures (Table 2). Furthermore, the quasi invariance of atomic density at ambient pressure with increasing S content (at least up to 30%at S) could suggest either a close similarity between Fe and S atomic radii (but this is not the case, as suggested by [*Stolz et al.*, 1994], Table 2) or is the result of a specific Fe-S interaction. In fact the large increase of compressibility with increasing S content (Figure 8), generated by the more compressible S atoms and the relatively constant value of the atomic density at low pressure with S content, reveals a non additive behaviour of the solution. However, to best reproduce the effect of S content on the compressibility using the NAHS model, we have to modify the HS diameter of pure Fe. Unfortunately, this adjustment significantly deteriorates the description of the EOS associated with pure liquid Fe (Figure 8). Nevertheless, this simple model has the ability to quantify the role of highly covalent bonding in the compressibility of Fe-S mixtures.

[34] As discussed previously the closure of the miscibility gap for Fe-S-Si with pressure seems to result from a structural similarity between Fe-S and Fe-Si liquid at high pressure. In fact, a recent investigation of the Fe-FeS eutectic up to 17 GPa concluded that the liquid structure evolves discontinuously toward a more compact structure at high pressure [*Morard et al.*, 2007b]. In terms of the HS fluid, this feature corresponds to a transition from a non-additive behaviour at low pressure to an additive one at high pressure (P > 15GPa).

[35] More generally, the structure factor S(Q) of some binary alloys can be reproduced quite satisfactorily by the AHS mixture model [*Ashcroft and Langreth*, 1966]. In the present case to constrain the HS diameters associated with liquid Fe-S alloys for P > 15 GPa, the structure factor obtained in a previous study [*Morard et al.*, 2007b] has been reproduced by using an analytic expression for $S^{AHS}(Q)$ (Figure 9), leading to σ_S = 1.9 Å and σ_{Fe} = 2.25 Å. The HS radius of Fe atoms is very close to the value (2.27 Å) used for describing the EOS of pure Fe, and that of S atoms corresponds approximately to the first peak of the pair distribution function observed in pure liquid S at ambient pressure [*Stolz et al.*, 1994] (Table 2) and is close to HS diameter of Si (σ_S = 2.08 Å) obtained from AHS model (Figure 7). Furthermore, the density so obtained (84 atoms/nm^3 for Fe-30%atS) is in good agreement with data from the literature [*Sanloup et al.*, 2000].

[36] Using these HS diameters, the additive HS model has been applied from P = 17 GPa up to core conditions (Figure 10). In this high pressure range, we observe a significant decrease of the compressibility with respect to the prediction made with the Birch-Murnaghan (BMEOS) fitted to experimental data at low and moderate pressure

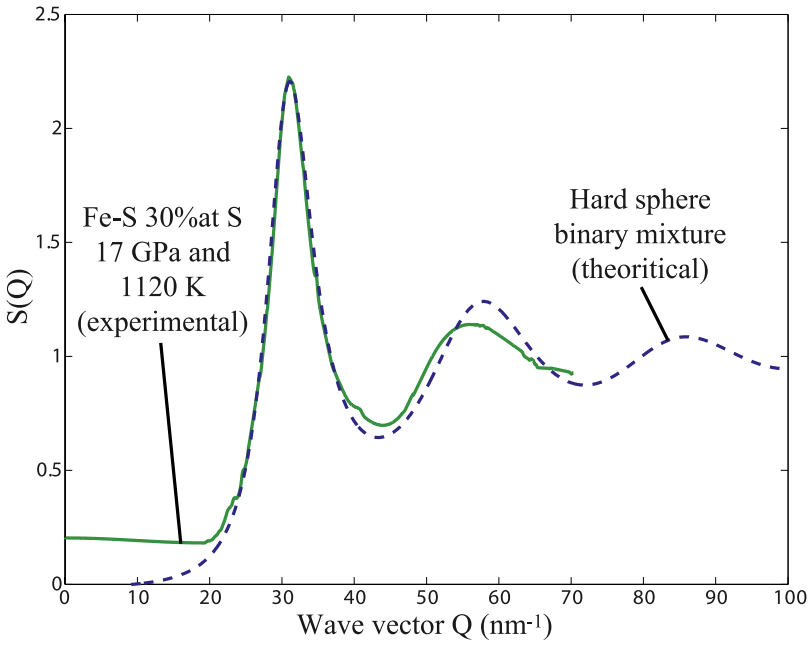

Figure 9. Structure factor S(Q) of the eutectic liquid Fe-20%wt S (Fe-30%at S) at 17 GPa and 1120 K (full line) [*Morard et al.*, 2007b] compared with HS binary mixture structure factor calculated using the analytical expression from *Ashcroft and Langreth* [1966] (dotted line). S(Q) simulation parameters are the following: $\eta = 0.442$; $\rho = 84$ atoms/nm^3; σFe = 2.25 Å; σS = 1.9 Å.

[*Sanloup et al.*, 2000]. A large value of the bulk modulus (K $\sim$ 60GPa) has been already established for Fe-10%wt S (16at% S) measured by sink-float method up to 20 GPa [*Balog et al.*, 2003].

[37] Although a more quantitative analysis using HS model is not possible under core conditions because the model does not account for the softness of electronic orbitals, some qualitative conclusions can be drawn (see below).

6. Geophysical Implications

[38] The presence of a large miscibility gap at moderate pressures (P < 15 GPa) is expected to have a direct influence on planetesimals and the core dynamics of small planets. For example, models of fractionated crystallisation processes in Ganymede's [*Hauck et al.*, 2006] and Mars' cores [*Stewart et al.*, 2007] should take into account the possibility of having an immiscible Si-rich metallic phase involved in the convection dynamics and its consequence on the geodynamo generation. In fact, S significantly affects the surface tension properties of iron alloys [*Lee and Morita*, 2002]. The immiscible liquid configuration observed in the hBN capsule (Figure 3) has also been observed with metal/silicate phases in coexistence [*Malavergne et al.*, 2007]. Therefore, an S-rich metallic phase could have acted as a geochemical buffer between silicates and Si-rich metallic phases in planetesimal cores. In this case, exchange between silicates and S-rich iron alloys would have a large influence on the pre-terrestrial geochemical balance.

[39] In contrast, the closure of the Fe-S-Si miscibility gap at high pressures is relevant for the Earth's core. In fact, the assessment that S and Si are not compatible in the same metallic phase during differentiation processes [*Kilburn and Wood*, 1997] has already been ruled out for P > 20 GPa [*Siebert et al.*, 2004]. Using the hypothesis of a differentiation equilibration of the metallic phase at the bottom of a magma ocean at pressure conditions well above 17 GPa (e.g. 27 GPa and 2200 K [*Righter et al.*, 1997]), we can deduce that the Earth's core could contain S and Si in appreciable amounts.

[40] A magnetic to non-magnetic transition occurs around 10–25 GPa in the Fe_3S compound [*Lin et al.*, 2004]. At the same time, the evolution of the c/a ratio in phase IV of FeS for P > 15 GPa indicates a metallization of the FeS compound [*Fei et al.*, 1995]. These findings are in agreement with an evolution of the Fe-S bond with increasing pressure from covalent to metallic. On the other hand, the solubility of S in solid Fe increases at P > 15 GPa [*Li et al.*, 2001], implying that S could act as an interstitial impurity and behaves like Si in liquid Fe at lower pressures.

[41] This evolution of the Fe-S interaction, from covalent to metallic appears to have a direct implication on the composition of the Earth's core. The way that S affects the sound velocity in liquid Fe is an argument that has been used to suggest that S is not one of the major light elements in the Earth's core [*Badro et al.*, 2007; *Sanloup et al.*, 2004]. As a matter of fact, in using density data on the Fe-S system in the pressure range 0–5 GPa, it has been argued [26] that the incorporation of S in liquid Fe would increase the discrepancy on the sound velocity with PREM. At variance with this conclusion, we calculate sound velocity Vp following equation:

$$Vp = \sqrt{\frac{K}{\rho}} \tag{4}$$

where K and ρ are respectively the compressibility and the density calculated from additive HS model under core

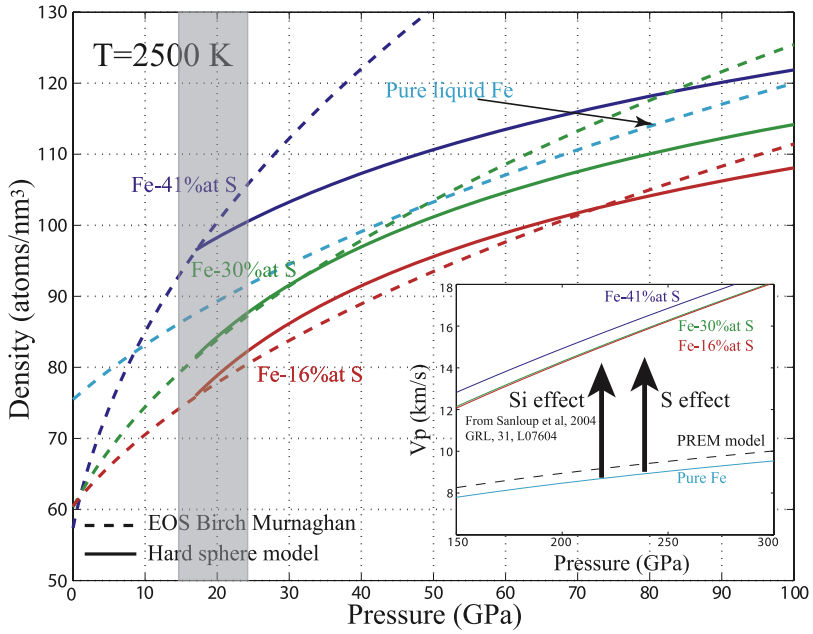

Figure 10. Additive HS EOS [*Mansoori et al.*, 1971] applied from 17 GPa to Fe-S alloys using HS diameter deduced from Figure 9. Shadow area indicates the pressure range where Fe-S liquid structure evolves toward a compact structure [*Morard et al.*, 2007b]. Inset shows calculated Vp for Fe-S alloys and pure liquid Fe using compressibility and density data deduced from additive HS model. The method used for Vp calculation is the same as *Sanloup and Fei* [2004].

conditions. Then, our calculations indicate that S drives the sound velocity toward the value of the PREM model (Figure 10, inset). Hence, S and Si will drive the sound velocity of liquid iron alloys in the same way, increasing it toward PREM values. So, from the standpoint of the elastic properties, S could be present in the Earth's core.

[42] More generally, this study indicates that it is not sufficient to interpret the differences in composition (e.g. S content) between the core of large planets, such as Earth or Venus, and planetesimals as a simple pressure effect. It is also important to consider two pressure domains, above or below ~15GPa, in order to distinguish between covalent and metallic behaviour for the incorporation of S into liquid Fe.

7. Conclusion

[43] In this study, the structural properties of immiscible Fe-S and Fe-Si liquid iron alloys have been investigated by in situ X-ray diffraction experiments. Large structural differences between coexisting liquids have been observed. These differences could be the origin of the Fe-S-Si miscibility gap observed at low and moderate pressures. However, by using in situ X-ray radiography we have shown that the Fe-S-Si system becomes miscible at high pressure. More precisely, the composition Fe-18wt%S-8.5wt%Si (Fe-28.8at%Si-11.9at%S) is found to be immiscible at 12 GPa but becomes miscible at 16 GPa. This evolution takes place in the same pressure range as the structural transition occurring in the binary alloy Fe-20at%S [*Morard et al.*, 2007b].

[44] The X-ray study of liquid Fe-S and liquid Fe-Si with comparable light element content provides an insight to explain the reason for a miscibility gap in Fe-S-Si system and its evolution with the pressure. In Fe-S mixtures at low and moderate pressures, the observation on the X-ray pair distribution function of a packing of the first coordination shell combined with a disordering of the second shell of neighbours is attributed to the covalent character of the Fe-S bond. In contrast Si behaves as an interstitial impurity in liquid Fe up to high Si content (oscillatory behaviour of the g(r)). Correspondingly the compressibility of Fe-S liquid is found to be much higher than that of liquid Fe-Si, a behaviour which is exacerbated when increasing S content [28]. At higher pressures (P > 15 GPa), the closure of the Fe-S-Si miscibility gap, the structural similarity noticed between Fe-S and Fe-Si liquids, and the large value reached by the bulk modulus of Fe-S liquid, all pleads in favour of a disappearance of the covalent character of the Fe-S bond with the pressure.

[45] As the Fe-S alloy adopts a compact structure similar to Fe-Si alloy for P > 17 GPa, we applied the additive HS model to describe qualitative behaviour of Fe-S alloy EOS under core conditions. The main result of this evaluation is a drastic increase of the bulk modulus, leading to the conclusion that S could be dissolved in appreciable amount in the Earth's core.

[46] **Acknowledgments.** We thank the ESRF staff of the High-Pressure Beamline ID27 (S. Bauchau and W. Crichton), and also the Spring8 staff of BL04B1 Beamline (Y. Tange).

[47] We also thank F. Coufignal and M. Fialin and the "centre de microanalyse Camparis" of UPMC (Paris) for the microprobe analysis.

References

Allègre, C. J., J. P. Poirier, E. Humler, and A. W. Hofmann (1995), The chemical composition of the Earth, *Earth Planet. Sci. Lett.*, *134*, 515–526.

Anderson, O. L., and T. J. Ahrens (1994), An equation of state for liquid iron and implications for the Earth's core, *J. Geophys. Res.*, *99*, 4273–4284.

Ashcroft, N. W., and D. C. Langreth (1966), Structure of binary liquid mixture. I, *Phys. Rev.*, *156*, 685–692.

Badro, J., G. Fiquet, F. Guyot, E. Gregoryanz, F. Occelli, D. Antonangeli, and M. D'Astuto (2007), Effect of light elements on the sound velocities in solid iron: Implications for the composition of Earth's core, *Earth Planet. Sci. Lett.*, *254*, 233–238.

Baker, J., M. Bizzarro, N. Wittig, J. Connelly, and H. Haack (2005), Early planetesimal melting from an age of 4.5662 Gyr for differenciated meteorites, *Nature*, *436*, 1127–1131.

Balog, P. S., R. A. Secco, D. C. Rubie, and D. J. Frost (2003), Equation of state of liquid Fe-10%wt S: Implications for the metallic cores of planetary bodies, *J. Geophys. Res.*, *108*(B2), 2124, doi:10.1029/2001JB001646.

Barker, J. A., and D. Henderson (1976), What is "liquid"? Understand the states of matter, *Rev. Modern Phys.*, *48*, 588–671.

Birch, F. (1952), Elasticity and constitution of the Earth's interior, *J. Geophys. Res.*, *57*, 227–286.

Boehler, R. (1992), Melting of the Fe-FeO and the Fe-FeS systems at high pressure: Constraints on core temperatures, *Earth Planet. Sci. Lett.*, *111*, 217–227.

Boehler, R., D. Errandonea, and M. Rossa (2002), Melting curve of iron: the never-ending story?, *High Pressure Res.*, *22*, 479–483.

Chabot, N. L., and H. Haack (2006), Evolution of asteroidal cores, in *Meteorites and the Early Solar System*, Univ. of Ariz. Press, Tucson.

Chudinovskikh, L., and R. Boehler (2007), Eutectic melting in the Fe-S system to 44 GPa, *Earth Planet. Sci. Lett.*, *257*, 97–103.

Delisle, A., D. J. Gonzalez, and M. J. Stott (2006), Pressure-induced structural and dynamical changes in liquid Si - an *ab initio* study, *J. Phys. Condens. Matter*, *18*, 3591–3605.

Dijkstra, M. (1998), Phase behaviour of nonadditive hard sphere mixtures, *Phys. Rev. E*, *58*, 7523–7528.

Faber, T. E., and J. M. Ziman (1965), A theory of electrical properties of liquid metals. 3. Resistivity of binary alloys, *Philos. Mag.*, *11*, 153.

Fabrichnaya, O. B., and B. Sundman (1997), The assesment of thermodynamics parameters in the Fe-O and Fe-Si-O systems, *Geochim. Cosmochim. Acta*, *61*, 4539–4555.

Fei, Y., C. M. Bertka, and L. W. Finger (1997), High pressure iron sulfur compound, Fe_3S_2, and melting relations in the Fe-FeS system, *Science*, *275*, 1621–1623.

Fei, Y., J. Li, C. M. Bertka, and C. T. Prewitt (2000), Structure type and bulk modulus of Fe3S, a new iron-sulfur compound, *Am. Mineral.*, *85*, 1830–1833.

Fei, Y., C. T. Prewitt, H. K. Mao, and C. M. Bertka (1995), Structure and density of FeS at high pressure and high temperature and the internal structure of Mars, *Science*, *268*, 1892–1894.

Greenwood, R. C., I. A. Franchi, A. Jambon, and P. C. Buchanan (2005), Widespread magma oceans on asteroidal bodies in the early Solar system, *Nature*, *435*, 916–918.

Grima, P., A. Polian, M. Gauthier, J. P. Itié, M. Mezouar, G. Weill, J. M. Besson, D. Haüsermann, and H. Hanfland (1995), Phase relationships in Mercury telluride under high temperature and pressure, *J. Phys. Chem. Solids*, *56*, 525–530.

Hamad, E. Z. (1997), Simulation and model testing of size asymmetric non-additive hard spheres, *Molecular Physics*, *91*, 371–375.

Hammersley, A. P., S. O. Svensson, H. Hanfland, A. N. Fitch, and D. Häusermann (1996), Two-dimensionnal detector software: from real detector to idealised image or two-theta scan, *High Pressure Res.*, *14*, 235–248.

Hauck, S. A., II, J. M. Aurnou, and A. J. Dombard (2006), Sulfur's impact on core evolution and magnetic field generation on Ganymede, *J. Geophys. Res.*, *111*, E09008, doi:10.1029/2005JE002557.

Iida, T., and R. I. L. Guthrie (1994), *The Physical Properties of the Liquid Metals*, Clarendon Press, Oxford.

Il'inskii, A., S. Slyusarenko, O. Slukhovskii, I. Kaban, and W. Hoyer (2002), Structural properties of liquid Fe-Si alloys, *J. Non Cryst. Sol.*, *306*, 90–98.

Javoy, M. (1995), The integral enstatite chondrite model of the Earth, *Geophys. Res. Lett.*, *22*, 2219–2222.

Jones, J. H., and D. J. Malvin (1990), A nonmetal interaction model for the segregation of trace metals during solidification of Fe-Ni-S, Fe-Ni-P and Fe-Ni-S-P alloys, *Metallurgical Trans. B*, *21*, 697–706.

Kilburn, M. R., and B. J. Wood (1997), Metal-silicate partitionning and the incompatibility of S and Si during core formation, *Earth Planet. Sci. Lett.*, *152*, 139–148.

Kita, Y., M. Zeze, and Z. Morita (1982), Structural analysis of molten Fe-Si alloys by X-ray diffraction, *Trans. Iron Steel Inst. Japan*, *22*, 571–576.

Kleine, T., K. Mezger, H. Palme, and C. Munker (2004), The W isotope evolution of the bulk silicate Earth: constraints on the timing and mechanisms of core formation and accretion, *Earth Planet. Sci. Lett.*, *228*, 109–123.

Kuwayama, Y., and K. Hirose (2004), Phase relations in the system Fe-FeSi at 21 GPa, *Am. Mineral.*, *89*, 273–276.

Le Godec, Y., D. Martinez-Garcia, M. Mezouar, G. Syfosse, J. P. Itie, and J. M. Besson (2000), Equation of state and order parameter in graphite-like hBN under high pressure and temperature, in *Science and Technology of High Pressure*, pp. 925–928, Universities Press, Hyderabad, India.

Lee, J., and K. Morita (2002), Evaluation of surface tension and adsorption for liquid Fe-S alloys, *ISIJ International*, *42*, 588–594.

Li, J., Y. Fei, H. K. Mao, K. Hirose, and S. R. Shieh (2001), Sulfur in the Earth's inner core, *Earth Planet. Sci. Lett.*, *193*, 509–514.

Lin, J. F., Y. Fei, W. Sturhahn, J. Zhao, H. K. Mao, and R. J. Hemley (2004), Magnetic transition and sound velocities of Fe_3S at high pressure: Implications for Earth and planetary cores, *Earth Planet. Sci. Lett.*, *226*, 33–40.

Lin, J. F., D. L. Heinz, A. J. Campbell, J. M. Devine, and G. Shen (2002), Iron-Silicon alloy in Earth's core?, *Science*, *295*, 313–315.

Malavergne, V., M. Tarrida, R. Combes, H. Bureau, J. Jones, and C. Schwandt (2007), New high-pressure and high-temperature metal/silicate partitioning of U and Pb: Implications for the cores of the Earth and Mars, *Geochim. Cosmochim. Acta*, *71*, 2637–2655.

Mansoori, G. A., N. F. Carnahan, K. E. Starling, and T. W. Leland (1971), Equilibrium thermodynamic properties of the mixture of hard spheres, *J. Chem. Phys.*, *54*, 1523–1525.

Mezouar, M., et al. (2005), Development of a new state-of-the-art beamline optimized for monochromatic single crystal and powder X-ray diffraction under extreme conditions at the ESRF, *J. Synch. Rad.*, *12*, 659–664.

Mezouar, M., P. Faure, W. A. Crichton, N. Rambert, B. Sitaud, S. Bauchau, and G. Blattman (2002), Multichannel collimator for structural investigation materials at high pressures and high temperatures, *Rev. Sci. Instr.*, *73*, 3570–3574.

Mezouar, M., T. Le Bihan, H. Libotte, Y. Le Godec, and D. Häusermann (1999), Paris-Edinburgh large volume cell coupled with a fast imaging-plate system for a structural investigation at high pressure and high temperature, *J. Synch. Rad.*, *6*, 1115–1119.

Mibe, K., M. Kanzaki, T. Kawamoto, K. N. Matsukage, Y. Fei, and S. Ono (2004), Determination of the second critical end point in silicate-H_2O systems using high-pressure and high-temperature X-ray radiography, *Geochim. Cosmochim. Acta*, *68*, 5189–5195.

Morard, G., D. Andrault, N. Guignot, C. Sanloup, M. Mezouar, S. Petitgirard, and G. Fiquet (2008), In-situ determination of Fe-Fe_3S phase diagram and liquid structural properties up to 65 GPa, *Earth Planet. Sci. Lett.*, in press.

Morard, G., et al. (2007a), Optimization of Paris Edinburgh cell assemblies for in situ monochromatic X-ray diffraction and X-ray absorption, *High Press. Res.*, *27*, 223–233.

Morard, G., C. Sanloup, G. Fiquet, M. Mezouar, N. Rey, R. Poloni, and P. Beck (2007b), Structure of eutectic Fe-FeS melts up to 17 GPa: Implications for planetary cores, *Earth Planet. Sci. Lett.*, *263*, 128–139.

Mulero, A., C. Galan, and F. Cuadros (2001), Equations of state for hard spheres. A review of accuracy and applications, *Phys. Chem. Chem. Phys.*, *3*, 4991–4999.

Ohtani, E., N. Hirao, T. Kondo, M. Ito, and T. Kikegawa (2005), Iron-water reaction at high pressure an temperature, and hydrogen transport to the core, *Phys. Chem. Minerals*, *32*, 77–82.

Ohtani, E., A. E. Ringwood, and W. Hibberson (1984), Composition of the core, II. Effect of high pressure on solubility of FeO in molten iron, *Earth Planet. Sci. Lett.*, *71*, 94–103.

Poirier, J. P. (1994), Light elements in the Earth's outer core: A critical review, *Phys. Earth Planet. Inter.*, *85*, 319–337.

Raghavan, V. (1988), Phase diagrams of ternary iron alloys. part 2: Ternary systems containing iron and sulphur Indian institute of metals, *Calcutta*, 270–278.

Righter, K., M. J. Drake, and G. Yaxley (1997), Prediction of siderophile element metal-silicate partition coefficients to 20 GPa and 2800°C: the effects of pressure, temperature, oxygen fugacity and silicate and metallic melt compositions, *Phys. Earth Planet. Inter.*, *100*, 115–134.

Sanloup, C. (2000), Contribution à l'étude de la structure interne de Mars. Expérimentation haute pression sur le fer liquide et ses alliages. Isotopes du zirconium dans les météorites., *Th., Ecole Normale Supérieure de Lyon*.

Sanloup, C., and Y. Fei (2004), Closure of the Fe-S-Si liquid miscibility gap at high pressure, *Phys. Earth Plan. Int.*, *147*, 57.

Sanloup, C., G. Fiquet, E. Gregoryanz, G. Morard, and M. Mezouar (2004), Effect of Si on liquid Fe compressibility: Implications for sound velocity in core materials, *Geophys. Res. Lett.*, *31*, L07604, doi:10.1029/2004GL019526.

Sanloup, C., F. Guyot, P. Gillet, and Y. Fei (2002), Physical properties of liquid Fe alloys at high pressure and their bearings on the nature of metallic planetary cores, *J. Geophys. Res.*, *107*(B11), 2272, doi:10.1029/2001JB000808.

Sanloup, C., F. Guyot, P. Gillet, M. Mezouar, and I. Martinez (2000), Density measurements on liquid Fe-S alloys at high pressure, *Geophys. Res. Lett.*, *27*, 811–814.

Sanloup, C., A. Jambon, and P. Gillet (1997), A simple chondritic model of Mars, *Phys. Earth Plan. Int.*, *112*, 43–54.

Santamaria-Perez, D., and R. Boehler (2008), FeSi melting curve up to 70 GPa, *Earth Planet. Sci. Lett.*, *265*, 743–747.

Seagle, C. T., D. L. Heinz, A. J. Campbell, V. B. Prakapenka, and S. T. Wanless (2008), Melting and thermal expansion in the Fe-FeO system at high pressure, *Earth Planet. Sci. Lett.*, *265*, 655–665.

Siebert, J., V. Malavergne, F. Guyot, R. Combe, and I. Martinez (2004), The behaviour of sulphur in metal-silicate core segregation under reducing conditions, *Phys. Earth Planet. Inter.*, *143–144*, 433–443.

Stewart, A. J., M. W. Schmidt, W. van Westrenen, and C. Liebske (2007), Mars: a new core-crystallisation regime, *Science*, *316*, 1323–1325.

Stolz, M., R. Winter, W. S. Howells, R. L. McGreevy, and P. A. Egelstaff (1994), The structural properties of liquid and quenched sulphur II, *J. Phys. Condens. Matter*, *6*, 3619–3628.

Tsuno, K., E. Ohtani, and H. Terasaki (2006), Immiscible two-liquid regions in the Fe-O-S system at high pressure: Implications for the planetary cores, *Phys. Earth Planet. Inter.*, *160*, 75–85.

Urakawa, S., N. Igawa, K. Kusaba, H. Ohno, and O. Shimomura (1998), Structure of molten iron sulfide under pressure, *Rev. High Press. Sci. Technol.*, *7*, 286–288.

Utsumi, W., K. Funakoshi, S. Urakawa, M. Yamakata, K. Tsuji, H. Konishi, and O. Shimomura (1998), SPring8 beamlines for high pressure science with multi-anvil apparatus, *Rev. High Press. Sci. Technol.*, *7*, 1484–1486.

Vineyard, G. H. (1958), Scattering of slow neutrons by a liquid, *Phys. Rev.*, *110*, 999–1010.

Vocadlo, L., D. Alfè, G. D. Price, and M. J. Gillan (2000), First principles calculations on the diffusivity and viscosity of liquid Fe-S at experimentally accessible conditions, *Phys. Earth Planet. Inter.*, *120*, 145–152.

Waseda, Y. (1980), *The Structure of Non-crystalline Materials*, McGraw-Hill, New York.

Wood, B. J. (1993), Carbon in the core, *Earth Planet. Sci. Lett.*, *117*, 593–607.

Yoshino, T., M. J. Walter, and T. Katsura (2003), Core formation in planetesimals triggered by permable flow, *Nature*, *422*, 154–157.

G. Fiquet, Institut de Minéralogie et de Physique des Milieux Condensés 140, rue de Lourmel, 75015 Paris, France.

K. Funakoshi, Spring-8, Japan Synchrotron Radiation Research Institute, 1-1-1, Kouto, Sayo-cho, Sayo-gun, Hyogo 679-5198 Japan.

G. Garbarino, M. Mezouar, and J. P. Perrillat, European Synchrotron Radiation Facility, 6 rue Jules Horowitz, BP220, 38043 Grenoble Cedex, France.

B. Guillot, Laboratoire de Physique Théorique de la Matière Condensée, Université Pierre et Marie Curie-Paris 6, UMR CNRS 7600, case 121, 4 Place Jussieu, F-75252 Paris, France.

T. Komabayashi, Department of Earth and Planetary Sciences, Tokyo Institute of Technology, 2-12-1 Okayama, Meguro, Tokyo 152-8551, Japan.

K. Mibe, Earthquake Research Institute, University of Tokyo, 1-1-1 Yayoi, Bunkyo-ku, Tokyo 113-0032, Japan.

G. Morard, Institute for Study of the Earth's Interior, 827 Yamada, Misasa, Tottori, 682-0193 Japan. (guillaume.morard@impmc.jussieu.fr)

C. Sanloup, Center for Science at Extreme Conditions and School of Geosciences, University of Edinburgh, Erskine Williamson Building, The King's Buildings, Mayfield Road, Edinburgh EH9 3JZ, UK.